

## **Supporting Information:**

Thermoelectrics with Earth Abundant Elements: Low thermal conductivity and high thermopower in doped SnS

Qing Tan,<sup>†</sup> Li-Dong Zhao,<sup>‡</sup> Jing-Feng Li,<sup>\*,†</sup> Chao-Feng Wu,<sup>†</sup> Tian-Ran Wei,<sup>†</sup> Zhi-Bo Xing<sup>†</sup> and  
Mercouri G. Kanatzidis<sup>\*,‡</sup>

<sup>†</sup>School of Materials Science and Engineering, State Key Laboratory of New Ceramics and Fine Processing, Tsinghua University, Beijing 100084, China

<sup>‡</sup>Department of Chemistry, Northwestern University, Evanston, Illinois 60208, United States

Corresponding Author: jingfeng@mail.tsinghua.edu.cn; m-kanatzidis@northwestern.edu

## Experimental details

**Synthesis:** Commercial powders of 99.9% Ag, 99.99% Sn and 99.99% S (Aladdin, Shanghai) were used as raw materials. The powders mixed with nominal compositions of SnS- $x\%$ Ag ( $x=0, 0.05, 0.25, 0.5, 1$  and  $2$ ) were synthesized using mechanical alloying (MA) at 450 rpm for 15 h in a purified argon ( $>99.5\%$ ) atmosphere. The MA-derived powders were consolidated by spark plasma sintering (Sumimoto SPS1050, Japan) at 933K in vacuum for 5 min under an axial pressure of 50 MPa, results in a pellets sample with dimension of  $\varnothing 15\text{mm}$  and 8mm thickness.

**Phase structures and microstructures:** The phase structures were examined by X-ray diffraction (XRD) using Cu K $\alpha$  radiation (D/max-2500, RIGAKU Japan). The morphologies of the bulk samples were observed by field-emission scanning electron microscopy (FESEM, LEO1530, Germany and JOEL JSM-7001F, Japan) and transmission electron microscopy (field emission TEM, JEM-2010F). Specimens used for TEM were polished to about 30-40  $\mu\text{m}$  and finally thinned to electron transparency using a precession ion-milling system at low angle (10-15  $^\circ$ ). High-resolution transmission electron microscopy (HRTEM) images of the pieces were recorded at 200 kV.

**Thermoelectric properties:** The Seebeck coefficient and electrical resistivity were measured using a Seebeck coefficient/electrical resistivity measuring systems (ZEM-2, Ulvac-Riko, Japan) at Tsinghua University of China and (ZEM-3, Ulvac-Riko, Japan) at Northwestern University of USA. The thermal conductivity was calculated by the relationship  $\kappa = DC_p\rho$ , where  $D$ ,  $C_p$  and  $\rho$  are the thermal diffusivity, heat capacity and the sample density, respectively. Thermal diffusivity  $D$  was measured by the laser flash method (TC9000, Ulvac-Riko, Japan) at Tsinghua University of China and (LFA457, Netzsch, Germany) at Northwestern University of USA; The thermal diffusivity  $D$  was measured along the same direction with that of electrical transport property using the same SPSeD samples. The  $C_p$  was determined by laser flash apparatus (LFA457, Netzsch, Germany) (Table S1 and Figure S1) and reconfirmed using physical property measurement system (PPMS) at the temperature ranges from 300 to 400 K; the sample density was measured by the Archimedes method (Table S2). The carrier concentration and mobility were measured using the Hall measurement system (ResiTest 8400, Toyo, Japan),

**X-ray photoelectron spectroscopy and band gaps:** The banding energy of polished SnS-1%Ag bulk was detected by the X-ray photoelectron spectroscopy (XPS, Escalab 250Xi; Thermo Scientific, UK).

**Band gap measurements:** Room-temperature optical diffuse reflectance measurements were performed on finely ground powders to probe the optical energy gap. The measurements were performed using a Shimadzu Model UV-3101PC double-beam, double-monochromator spectrophotometer (ultraviolet-visible absorption spectroscopy). BaSO<sub>4</sub> was used as a 100%

reflectance standard. The generated reflectance versus wavelength data were used to estimate the bandgap by converting reflectance to absorption data according to the Kubelka-Munk equation:  $\alpha/S = (1 - R)^2/(2R)$ , where  $R$  is the reflectance, and  $\alpha$  and  $S$  are the absorption and scattering coefficients, respectively.

## 1. The heat capacity and thermal diffusivity

To confirm the heat capacity ( $C_p$ ) in this work is precise,  $C_p$  was re-measured using the physical property measurement system (PPMS) at the temperature ranges from 300 to 400 K, the results show good consistent with those measured by the laser flash apparatus (LFA457, Netzsch, Germany). The  $C_p$  values at room temperature measured by different methods are consistent with the Dulong-Petit limit  $0.331 \text{ J g}^{-1} \text{ K}^{-1}$ , these values at room temperature also show a good agreement with the reported value of  $0.34 \text{ J g}^{-1} \text{ K}^{-1}$  [ref. S1]. The heat capacity values for SnS are listed in Table S1. The thermal diffusivity and  $C_p$  values are shown in Figure S1.

**Table S1** The heat capacity of SnS measured by different methods

Temperature/K	~300	325	350	375	400
PPMS	0.32	0.331	0.339	0.352	0.359
Laser flash	0.341	0.348	-	0.357	-
D-T limit	0.331				
Ref. S1		0.34			

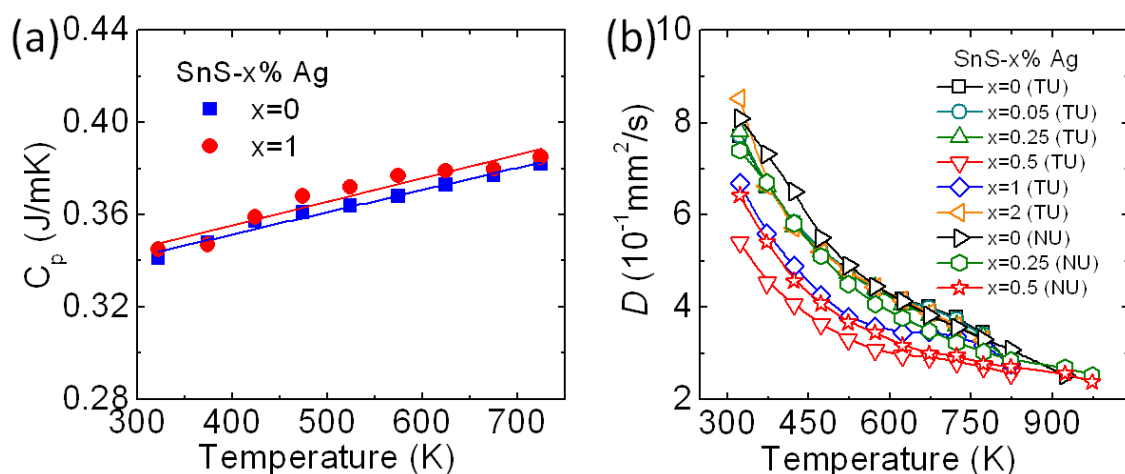


**Figure S1** Temperature dependence of (a) thermal diffusivity of SnS-x% Ag ( $x=0, 0.05, 0.25, 0.5, 1$  and  $2$ ) and (b) Temperature dependence of  $C_p$  heat capacity of SnS and SnS-1%Ag. TU represents the results measured at Tsinghua University of China, and the NU represents the results measured at Northwestern University of USA.

## 2. Samples density

**Table S2** The sample density of SnS-x%Ag ( $x=0, 0.05, 0.25, 0.5, 1$  and  $2$ ).

$x$	Density(g/m <sup>3</sup> )
0	4.98
0.05%	4.89
0.25%	4.85
0.5%	4.88
1%	5.05
2%	5.03

### 3. Experimental repeatability

To ensure the experimental repeatability, three compositions, SnS, SnS-0.25%Ag, SnS-0.5%Ag samples, were re-measured at Northwestern University (NU). All the data are comparable, indicating that the results in different groups show good agreements. In the main context, the average values were taken, as the thick solid line shown in Figure S2.

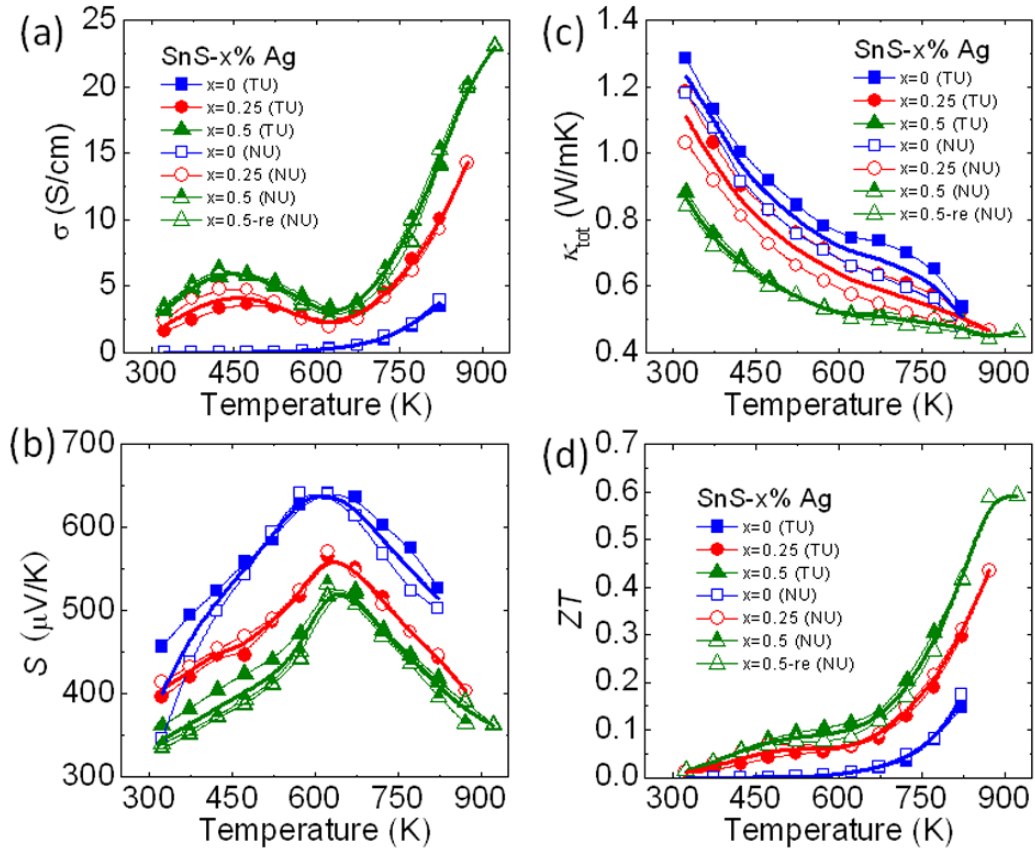


**Figure S2** Temperature dependence of (a) electrical conductivity (b) Seebeck coefficient (c) thermal conductivity and (d)  $ZT$  of the undoped SnS (blue), 0.25%Ag-SnS (red) and 0.5%Ag (green) bulks. TU represents the results measured at Tsinghua University of China, and the NU represents the results measured at Northwestern University of USA.

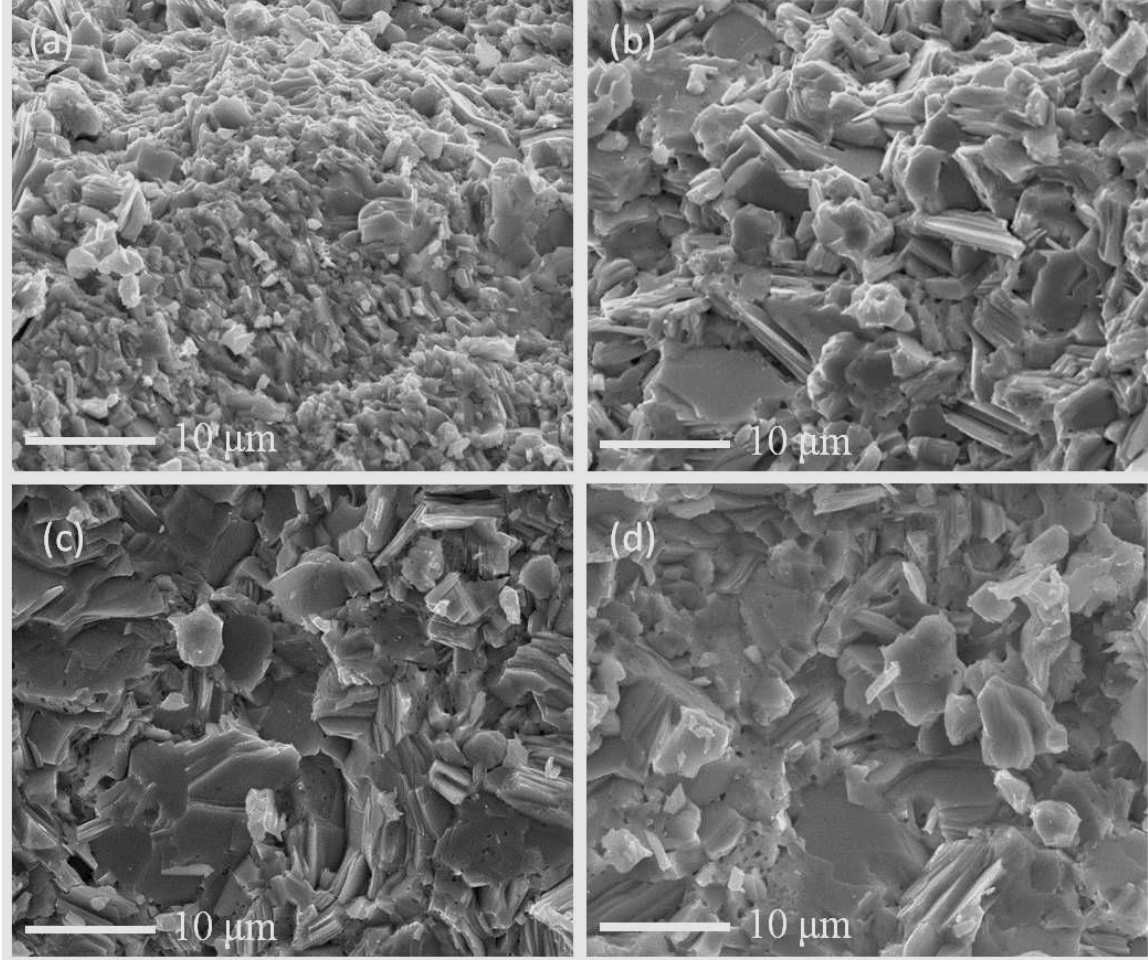


**Figure S3** FESEM images of of SnS- $x\%$ Ag ( $x = 0, 0.5, 1$  and  $2$ ) samples: (a)  $x=0$ , (b)  $x=0.5$ , (c)  $x=1$ , (d)  $x=2$ .

#### 4. Calculation details

As mentioned in the context, the scattering factors ( $s$ ) are  $-3/2$ ,  $-1/2$ ,  $3/2$  and  $0$  for the optical phonon, acoustic phonon, ionized impurity and constant scattering time mechanism, respectively.  $s$  of  $3/2$  was used at room temperature because the ionized impurity scattering was assumed to be the main carrier scattering mechanism according to the measurements and calculations in the main context.

Generally,  $\kappa$  is composed of two components:

$$\kappa = \kappa_e + \kappa_L = L\sigma T + \kappa_L \quad (\text{S1})$$

where  $\kappa_e$  is the electronic thermal conductivity,  $\kappa_L$  is the lattice thermal conductivity,  $L$  is the Lorenz factor,  $\sigma$  is the electrical conductivity and  $T$  is the absolute temperature.  $L$  can be calculated using:

$$L = \left(\frac{k_B}{e}\right)^2 \left\{ \frac{(s+7/2)F_{s+5/2}(\eta)}{(s+3/2)F_{s+1/2}(\eta)} - \left[ \frac{(s+5/2)F_{s+3/2}(\eta)}{(s+3/2)F_{s+1/2}(\eta)} \right]^2 \right\} \quad (\text{S2})$$

where  $s$  was  $3/2$  at 323 K and  $-1/2$  at 873 K. The determination of  $s$  is explained as follows.

According to the previous researches (for example, P. Y. Yu, M. Cardona, *Fundamentals of Semiconductors Physics and Materials Properties*, Springer, Berlin, **1999**, pp. 210-212.), one can determine the contributions from the different scattering mechanisms by comparing the measured temperature dependence of the mobility with theory. The relationship between  $\ln \mu$  and  $\ln T$  for the SnS and  $\text{Sn}_{0.995}\text{Ag}_{0.005}\text{S}$  samples are plotted as Figure S4 shown. It can be divided to three zones. From left to right is Zone I, the transitional zone, and Zone II. Zone I ranges from 323 to 423 K and Zone II ranges from 523 to 673 K, where both of the curves were linearly fitted. The slopes were the scattering factor, as displayed in Figure S4, where  $s_{0,I}$ ,  $s_{Ag,I}$ ,  $s_{0,II}$  and  $s_{Ag,II}$  are the fitting liner slopes for the SnS and  $\text{Ag}_{0.005}\text{Sn}_{0.995}\text{S}$  samples in Zone I and Zone II, respectively. The  $s_{0,I}$  and  $s_{Ag,I}$  were  $\approx 3/2$ , suggesting that the scattering of the charge carriers in SnS and  $\text{Sn}_{0.995}\text{Ag}_{0.005}\text{S}$  were dominated by ionized impurities in Zone I.  $s_{0,II}$  and  $s_{Ag,II}$  were close to 0 and  $-3/2$ , respectively, indicating that the constant scattering time mechanism played the most important role in SnS and acoustic phonon scattering was the main scattering mechanism in  $\text{Sn}_{0.995}\text{Ag}_{0.005}\text{S}$  in Zone II. Thus the  $s$  was considered as  $3/2$  at 323 K and  $-1/2$  at 873 K. In addition, the value of  $s$  have no effects on the trend of the effective mass among samples.

The effective mass  $m^*$  was calculated using the following equations, when the scattering factor had been determined:

$$\begin{aligned} S &= \pm \frac{k_B}{e} \left[ \frac{(s + 5/2) F_{s+3/2}(\eta)}{(s + 3/2) F_{s+1/2}(\eta)} - \eta \right] \\ &= \frac{k_B}{e} \left[ \left( s + \frac{5}{2} \right) + \ln \frac{2(2\pi m^* k_B T)^{3/2}}{n h^3} \right] \quad (\text{nondegenerate limit}) \end{aligned} \quad (\text{S3})$$

$$n = 4\pi \left( \frac{2m^* k_B T}{h^2} \right)^{3/2} \frac{F_{1/2}(\eta)}{r_H} \quad (\text{S4})$$

In equations (1) and (2)  $\eta$  is the reduced Fermi energy,  $F_n(\eta)$  is the  $n$ th order Fermi integral,  $k_B$  is Boltzmann's constant,  $h$  is Planck's constant and  $r_H$  is the Hall coefficient.

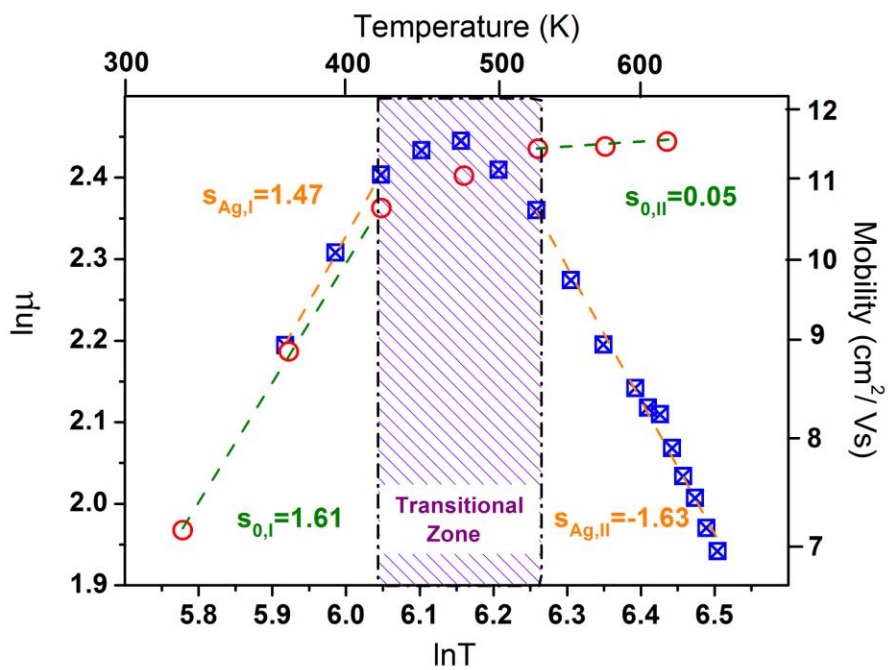


**Figure S4** Temperature dependence of Mobility

## References:

- [S1]. D. L. Ye, *Thermodynamics Manual of Practical Inorganic*, Metallurgical Industry, Beijing, China, **2002**, pp. 516-519